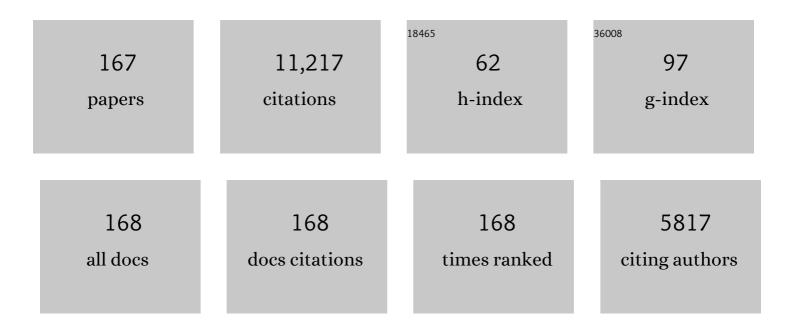
List of Publications by Year in descending order

Source: https://exaly.com/author-pdf/369535/publications.pdf Version: 2024-02-01



VUE DENC

#	Article	IF	CITATIONS
1	Comparative study of α-, β-, γ- and δ-MnO2 on toluene oxidation: Oxygen vacancies and reaction intermediates. Applied Catalysis B: Environmental, 2020, 260, 118150.	10.8	400
2	Novel effect of SO2 on the SCR reaction over CeO2: Mechanism and significance. Applied Catalysis B: Environmental, 2013, 136-137, 19-28.	10.8	312
3	Identification of the active sites on CeO2–WO3 catalysts for SCR of NOx with NH3: An in situ IR and Raman spectroscopy study. Applied Catalysis B: Environmental, 2013, 140-141, 483-492.	10.8	295
4	Perfluorooctanoic Acid Degradation Using UV–Persulfate Process: Modeling of the Degradation and Chlorate Formation. Environmental Science & Technology, 2016, 50, 772-781.	4.6	294
5	Removal of Antimonite (Sb(III)) and Antimonate (Sb(V)) from Aqueous Solution Using Carbon Nanofibers That Are Decorated with Zirconium Oxide (ZrO ₂). Environmental Science & Technology, 2015, 49, 11115-11124.	4.6	233
6	Roles of Oxygen Vacancies in the Bulk and Surface of CeO ₂ for Toluene Catalytic Combustion. Environmental Science & Technology, 2020, 54, 12684-12692.	4.6	231
7	Mechanism of N ₂ O Formation during the Low-Temperature Selective Catalytic Reduction of NO with NH ₃ over Mn–Fe Spinel. Environmental Science & Technology, 2014, 48, 10354-10362.	4.6	225
8	Alkali Metal Poisoning of a CeO ₂ –WO ₃ Catalyst Used in the Selective Catalytic Reduction of NO _{<i>x</i>} with NH ₃ : an Experimental and Theoretical Study. Environmental Science & Technology, 2012, 46, 2864-2869.	4.6	200
9	Selective Dissolution of Aâ€Site Cations in ABO ₃ Perovskites: A New Path to Highâ€Performance Catalysts. Angewandte Chemie - International Edition, 2015, 54, 7954-7957.	7.2	180
10	Deactivation and regeneration of a commercial SCR catalyst: Comparison with alkali metals and arsenic. Applied Catalysis B: Environmental, 2015, 168-169, 195-202.	10.8	180
11	Fe–Ti spinel for the selective catalytic reduction of NO with NH3: Mechanism and structure–activity relationship. Applied Catalysis B: Environmental, 2012, 117-118, 73-80.	10.8	178
12	Dispersion of tungsten oxide on SCR performance of V2O5WO3/TiO2: Acidity, surface species and catalytic activity. Chemical Engineering Journal, 2013, 225, 520-527.	6.6	177
13	Efficient Electrochemical Nitrate Reduction to Ammonia with Copperâ€Supported Rhodium Cluster and Singleâ€Atom Catalysts. Angewandte Chemie - International Edition, 2022, 61, .	7.2	170
14	A high-efficiency γ-MnO ₂ -like catalyst in toluene combustion. Chemical Communications, 2015, 51, 14977-14980.	2.2	153
15	Mechanism of arsenic poisoning on SCR catalyst of CeW/Ti and its novel efficient regeneration method with hydrogen. Applied Catalysis B: Environmental, 2016, 184, 246-257.	10.8	149
16	Structure–activity relationship of VOx/CeO2 nanorod for NO removal with ammonia. Applied Catalysis B: Environmental, 2014, 144, 538-546.	10.8	144
17	Deactivation Mechanism of Potassium on the V ₂ O ₅ /CeO ₂ Catalysts for SCR Reaction: Acidity, Reducibility and Adsorbed-NO _{<i>x</i>} . Environmental Science & Technology, 2014, 48, 4515-4520.	4.6	137
18	Novel nanowire self-assembled hierarchical CeO2 microspheres for low temperature toluene catalytic combustion. Chemical Engineering Journal, 2018, 331, 425-434.	6.6	135

#	Article	IF	CITATIONS
19	Design Strategies for Development of SCR Catalyst: Improvement of Alkali Poisoning Resistance and Novel Regeneration Method. Environmental Science & Technology, 2012, 46, 12623-12629.	4.6	134
20	Controllable redox-induced in-situ growth of MnO2 over Mn2O3 for toluene oxidation: Active heterostructure interfaces. Applied Catalysis B: Environmental, 2020, 278, 119279.	10.8	131
21	Templateâ€free Scalable Synthesis of Flowerâ€like Co _{3â€<i>x</i>} Mn _{<i>x</i>} O ₄ Spinel Catalysts for Toluene Oxidation. ChemCatChem, 2018, 10, 3429-3434.	1.8	125
22	Low content of CoOx supported on nanocrystalline CeO2 for toluene combustion: The importance of interfaces between active sites and supports. Applied Catalysis B: Environmental, 2019, 240, 329-336.	10.8	124
23	The role of the Cu dopant on a Mn3O4 spinel SCR catalyst: Improvement of low-temperature activity and sulfur resistance. Chemical Engineering Journal, 2020, 387, 124090.	6.6	124
24	Comparison of MoO3 and WO3 on arsenic poisoning V2O5/TiO2 catalyst: DRIFTS and DFT study. Applied Catalysis B: Environmental, 2016, 181, 692-698.	10.8	117
25	Multipollutant Control (MPC) of Flue Gas from Stationary Sources Using SCR Technology: A Critical Review. Environmental Science & Technology, 2021, 55, 2743-2766.	4.6	117
26	De-reducibility mechanism of titanium on maghemite catalysts for the SCR reaction: An in situ DRIFTS and quantitative kinetics study. Applied Catalysis B: Environmental, 2018, 221, 556-564.	10.8	116
27	The relationship between structure and activity of MoO3–CeO2 catalysts for NO removal: influences of acidity and reducibility. Chemical Communications, 2013, 49, 6215.	2.2	113
28	Enhanced low-temperature activity of LaMnO3 for toluene oxidation: The effect of treatment with an acidic KMnO4. Chemical Engineering Journal, 2019, 366, 92-99.	6.6	112
29	Ammonia adsorption on graphene and graphene oxide: a first-principles study. Frontiers of Environmental Science and Engineering, 2013, 7, 403-411.	3.3	111
30	Facile surface improvement method for LaCoO ₃ for toluene oxidation. Catalysis Science and Technology, 2018, 8, 3166-3173.	2.1	111
31	The effect of SiO2 on a novel CeO2–WO3/TiO2 catalyst for the selective catalytic reduction of NO with NH3. Applied Catalysis B: Environmental, 2013, 140-141, 276-282.	10.8	110
32	Surface Tuning of La _{0.5} Sr _{0.5} CoO ₃ Perovskite Catalysts by Acetic Acid for NO _{<i>x</i>} Storage and Reduction. Environmental Science & Technology, 2016, 50, 6442-6448.	4.6	108
33	Investigation of the Poisoning Mechanism of Lead on the CeO ₂ —WO ₃ Catalyst for the NH ₃ –SCR Reaction via in Situ IR and Raman Spectroscopy Measurement. Environmental Science & Technology, 2016, 50, 9576-9582.	4.6	106
34	Using Transient FTIR Spectroscopy to Probe Active Sites and Reaction Intermediates for Selective Catalytic Reduction of NO on Cu/SSZ-13 Catalysts. ACS Catalysis, 2019, 9, 6137-6145.	5.5	105
35	Investigation on a novel CaO–Y2O3 sorbent for efficient CO2 mitigation. Chemical Engineering Journal, 2014, 243, 297-304.	6.6	103
36	Comparison on the Performance of α-Fe2O3 and γ-Fe2O3 for Selective Catalytic Reduction of Nitrogen Oxides with Ammonia. Catalysis Letters, 2013, 143, 697-704.	1.4	101

YUE PENG

#	Article	IF	CITATIONS
37	Low temperature complete combustion of methane over cobalt chromium oxides catalysts. Catalysis Today, 2013, 201, 12-18.	2.2	100
38	Chemical poison and regeneration of SCR catalysts for NO x removal from stationary sources. Frontiers of Environmental Science and Engineering, 2016, 10, 413-427.	3.3	100
39	Insight into Deactivation of Commercial SCR Catalyst by Arsenic: An Experiment and DFT Study. Environmental Science & Technology, 2014, 48, 13895-13900.	4.6	98
40	Ceria promotion on the potassium resistance of MnOx/TiO2 SCR catalysts: An experimental and DFT study. Chemical Engineering Journal, 2015, 269, 44-50.	6.6	92
41	Substitution of WO ₃ in V ₂ O ₅ /WO ₃ –TiO ₂ by Fe ₂ O ₃ for selective catalytic reduction of NO with NH3. Catalysis Science and Technology, 2013, 3, 161-168.	2.1	90
42	Synthesis, characterization, and catalytic evaluation of Co 3 O 4 \hat{I}^3 -Al 2 O 3 as methane combustion catalysts: Significance of Co species and the redox cycle. Applied Catalysis B: Environmental, 2015, 168-169, 42-50.	10.8	90
43	Impacts of Pb and SO ₂ Poisoning on CeO ₂ –WO ₃ /TiO ₂ –SiO ₂ SCR Catalyst. Environmental Science & Technology, 2017, 51, 11943-11949.	4.6	90
44	Regeneration of Commercial SCR Catalysts: Probing the Existing Forms of Arsenic Oxide. Environmental Science & Technology, 2015, 49, 9971-9978.	4.6	89
45	Reaction Pathway Investigation on the Selective Catalytic Reduction of NO with NH ₃ over Cu/SSZ-13 at Low Temperatures. Environmental Science & amp; Technology, 2015, 49, 467-473.	4.6	87
46	Different exposed facets VO /CeO2 catalysts for the selective catalytic reduction of NO with NH3. Chemical Engineering Journal, 2018, 349, 184-191.	6.6	86
47	The deactivation mechanism of toluene on MnOx-CeO2 SCR catalyst. Applied Catalysis B: Environmental, 2020, 277, 119257.	10.8	86
48	Superior Oxidative Dehydrogenation Performance toward NH ₃ Determines the Excellent Low-Temperature NH ₃ -SCR Activity of Mn-Based Catalysts. Environmental Science & Technology, 2021, 55, 6995-7003.	4.6	83
49	The poisoning mechanism of gaseous HCl on low-temperature SCR catalysts: MnO â^CeO2 as an example. Applied Catalysis B: Environmental, 2020, 267, 118668.	10.8	82
50	Alloying effect-induced electron polarization drives nitrate electroreduction to ammonia. Chem Catalysis, 2021, 1, 1088-1103.	2.9	80
51	NH3-SCR performance of WO3 blanketed CeO2 with different morphology: Balance of surface reducibility and acidity. Catalysis Today, 2019, 332, 42-48.	2.2	79
52	Correlation of the changes in the framework and active Cu sites for typical Cu/CHA zeolites (SSZ-13) Tj ETQq0 0	0 rgBT /O\ 1.3	verlock 10 Tf
53	Non-thermal plasma catalysis for chlorobenzene removal over CoMn/TiO2 and CeMn/TiO2: Synergistic effect of chemical catalysis and dielectric constant. Chemical Engineering Journal, 2018, 347, 447-454.	6.6	76

⁵⁴Performance and Mechanism of Photocatalytic Toluene Degradation and Catalyst Regeneration by
Thermal/UV Treatment. Environmental Science & amp; Technology, 2020, 54, 14465-14473.4.676

#	Article	IF	CITATIONS
55	Deactivation Mechanism of Multipoisons in Cement Furnace Flue Gas on Selective Catalytic Reduction Catalysts. Environmental Science & Technology, 2019, 53, 6937-6944.	4.6	75
56	Synergistic Promotion Effect between NO _{<i>x</i>} and Chlorobenzene Removal on MnO _{<i>x</i>} –CeO ₂ Catalyst. ACS Applied Materials & Interfaces, 2018, 10, 30426-30432.	4.0	74
57	Extraordinary Deactivation Offset Effect of Arsenic and Calcium on CeO ₂ –WO ₃ SCR Catalysts. Environmental Science & Technology, 2018, 52, 8578-8587.	4.6	73
58	Interaction of phosphorus with a FeTiOx catalyst for selective catalytic reduction of NOx with NH3: Influence on surface acidity and SCR mechanism. Chemical Engineering Journal, 2018, 347, 173-183.	6.6	72
59	Theory and practice of metal oxide catalyst design for the selective catalytic reduction of NO with NH3. Catalysis Today, 2021, 376, 292-301.	2.2	71
60	Boosting the Catalytic Performance of CeO ₂ in Toluene Combustion via the Ce–Ce Homogeneous Interface. Environmental Science & Technology, 2021, 55, 12630-12639.	4.6	71
61	Structural effects of iron spinel oxides doped with Mn, Co, Ni and Zn on selective catalytic reduction of NO with NH3. Journal of Molecular Catalysis A, 2013, 376, 13-21.	4.8	68
62	Performance of Modified La _{<i>x</i>} Sr _{1–<i>x</i>} MnO ₃ Perovskite Catalysts for NH ₃ Oxidation: TPD, DFT, and Kinetic Studies. Environmental Science & Technology, 2018, 52, 7443-7449.	4.6	67
63	Selective catalytic reduction of NO with NH ₃ over novel iron–tungsten mixed oxide catalyst in a broad temperature range. Catalysis Science and Technology, 2015, 5, 4556-4564.	2.1	65
64	Comparison of the Structures and Mechanism of Arsenic Deactivation of CeO ₂ –MoO ₃ and CeO ₂ –WO ₃ SCR Catalysts. Journal of Physical Chemistry C, 2016, 120, 18005-18014.	1.5	64
65	Probing Active-Site Relocation in Cu/SSZ-13 SCR Catalysts during Hydrothermal Aging by In Situ EPR Spectroscopy, Kinetics Studies, and DFT Calculations. ACS Catalysis, 2020, 10, 9410-9419.	5.5	64
66	Dechlorination of chlorobenzene on vanadium-based catalysts for low-temperature SCR. Chemical Communications, 2018, 54, 2032-2035.	2.2	63
67	Characterization of CeO2–WO3 catalysts prepared by different methods for selective catalytic reduction of NO with NH3. Catalysis Communications, 2013, 40, 145-148.	1.6	61
68	Ultra hydrothermal stability of CeO2-WO3/TiO2 for NH3-SCR of NO compared to traditional V2O5-WO3/TiO2 catalyst. Catalysis Today, 2015, 258, 11-16.	2.2	61
69	Hollow-Structural Ag/Co ₃ O ₄ Nanocatalyst for CO Oxidation: Interfacial Synergistic Effect. ACS Applied Nano Materials, 2019, 2, 3480-3489.	2.4	60
70	Selective Dissolution of Aâ€Site Cations in ABO ₃ Perovskites: A New Path to Highâ€Performance Catalysts. Angewandte Chemie, 2015, 127, 8065-8068.	1.6	58
71	Sn-doped rutile TiO2 for vanadyl catalysts: Improvements on activity and stability in SCR reaction. Applied Catalysis B: Environmental, 2020, 269, 118797.	10.8	57
72	Dextrose-aided hydrothermal preparation with large surface area on 1D single-crystalline perovskite La0.5Sr0.5CoO3 nanowires without template: Highly catalytic activity for methane combustion. Journal of Molecular Catalysis A, 2013, 378, 299-306.	4.8	56

#	Article	lF	CITATIONS
73	Studies on toluene adsorption performance and hydrophobic property in phenyl functionalized KIT-6. Chemical Engineering Journal, 2018, 334, 191-197.	6.6	56
74	Manganese doped CeO2–WO3 catalysts for the selective catalytic reduction of NO with NH3: An experimental and theoretical study. Catalysis Communications, 2012, 19, 127-131.	1.6	55
75	Multi-pollutant control (MPC) of NO and chlorobenzene from industrial furnaces using a vanadia-based SCR catalyst. Applied Catalysis B: Environmental, 2021, 285, 119835.	10.8	54
76	Intra-crystalline mesoporous zeolite encapsulation-derived thermally robust metal nanocatalyst in deep oxidation of light alkanes. Nature Communications, 2022, 13, 295.	5.8	54
77	A novel magnetic Fe–Ti–V spinel catalyst for the selective catalytic reduction of NO with NH3 in a broad temperature range. Catalysis Science and Technology, 2012, 2, 915.	2.1	53
78	Surface In Situ Doping Modification over Mn ₂ O ₃ for Toluene and Propene Catalytic Oxidation: The Effect of Isolated Cu ^{δ+} Insertion into the Mezzanine of Surface MnO ₂ Cladding. ACS Applied Materials & Interfaces, 2021, 13, 2753-2764.	4.0	53
79	Photothermal Synergistic Effect of Pt ₁ /CuO-CeO ₂ Single-Atom Catalysts Significantly Improving Toluene Removal. Environmental Science & Technology, 2022, 56, 8722-8732.	4.6	52
80	Effects of noble metals doped on mesoporous <scp>LaAlNi</scp> mixed oxide catalyst and identification of carbon deposit for reforming <scp>CH₄</scp> with <scp>CO₂</scp> . Journal of Chemical Technology and Biotechnology, 2014, 89, 372-381.	1.6	51
81	An experimental and DFT study of the adsorption and oxidation of NH3 on a CeO2 catalyst modified by Fe, Mn, La and Y. Catalysis Today, 2015, 242, 300-307.	2.2	51
82	Core-shell-like structured α-MnO2@CeO2 catalyst for selective catalytic reduction of NO: Promoted activity and SO2 tolerance. Chemical Engineering Journal, 2020, 391, 123473.	6.6	50
83	Identification of the reaction pathway and reactive species for the selective catalytic reduction of NO with NH ₃ over cerium–niobium oxide catalysts. Catalysis Science and Technology, 2016, 6, 2136-2142.	2.1	49
84	MnO -CeO2 catalysts for effective NO reduction in the presence of chlorobenzene. Catalysis Communications, 2018, 117, 1-4.	1.6	49
85	Balance of activation and ring-breaking for toluene oxidation over CuO-MnO bimetallic oxides. Journal of Hazardous Materials, 2021, 415, 125637.	6.5	49
86	Experimental and DFT studies on Sr-doped LaMnO ₃ catalysts for NO _x storage and reduction. Catalysis Science and Technology, 2015, 5, 2478-2485.	2.1	48
87	Interaction Mechanism for Simultaneous Elimination of Nitrogen Oxides and Toluene over the Bifunctional CeO ₂ –TiO ₂ Mixed Oxide Catalyst. Environmental Science & Technology, 2022, 56, 4467-4476.	4.6	47
88	Dual Active Centers Bridged by Oxygen Vacancies of Ruthenium Singleâ€Atom Hybrids Supported on Molybdenum Oxide for Photocatalytic Ammonia Synthesis. Angewandte Chemie - International Edition, 2022, 61, .	7.2	45
89	Inhibition Effect of Phosphorus Poisoning on the Dynamics and Redox of Cu Active Sites in a Cu-SSZ-13 NH ₃ -SCR Catalyst for NO <i>_x</i> Reduction. Environmental Science & Technology, 2021, 55, 12619-12629.	4.6	43
90	Electronic structure tailoring of Al3+- and Ta5+-doped CeO2 for the synergistic removal of NO and chlorinated organics. Applied Catalysis B: Environmental, 2022, 304, 120939.	10.8	42

#	Article	IF	CITATIONS
91	A multiple-active-site Cu/SSZ-13 for NH3-SCO: Influence of Si/Al ratio on the catalytic performance. Catalysis Communications, 2020, 135, 105751.	1.6	40
92	Engineering surface functional groups on mesoporous silica: towards a humidity-resistant hydrophobic adsorbent. Journal of Materials Chemistry A, 2018, 6, 13769-13777.	5.2	39
93	The synergistic mechanism of NO _x and chlorobenzene degradation in municipal solid waste incinerators. Catalysis Science and Technology, 2019, 9, 4286-4292.	2.1	39
94	Fe-Doped α-MnO ₂ nanorods for the catalytic removal of NO _x and chlorobenzene: the relationship between lattice distortion and catalytic redox properties. Physical Chemistry Chemical Physics, 2019, 21, 25880-25888.	1.3	39
95	The relationship between surface open cells of α-MnO ₂ and CO oxidation ability from a surface point of view. Journal of Materials Chemistry A, 2017, 5, 20911-20921.	5.2	38
96	A new insight into adsorption state and mechanism of adsorbates in porous materials. Journal of Hazardous Materials, 2020, 382, 121103.	6.5	38
97	Like Cures like: Detoxification Effect between Alkali Metals and Sulfur over the V ₂ O ₅ /TiO ₂ deNO _{<i>x</i>} Catalyst. Environmental Science & Technology, 2022, 56, 3739-3747.	4.6	38
98	Impact of NOx and NH3 addition on toluene oxidation over MnOx-CeO2 catalyst. Journal of Hazardous Materials, 2021, 416, 125939.	6.5	37
99	Balance between Reducibility and N ₂ O Adsorption Capacity for the N ₂ O Decomposition: Cu _{<i>x</i>} Co _{<i>y</i>} Catalysts as an Example. Environmental Science & Technology, 2019, 53, 10379-10386.	4.6	36
100	Highly selective α-Mn2O3 catalyst for cGPF soot oxidation: Surface activated oxygen enhancement via selective dissolution. Chemical Engineering Journal, 2019, 364, 448-451.	6.6	35
101	The promotional effect of MoO3 doped V2O5/TiO2 for chlorobenzene oxidation. Catalysis Communications, 2015, 69, 161-164.	1.6	34
102	Revealing the Synergistic Deactivation Mechanism of Hydrothermal Aging and SO ₂ Poisoning on Cu/SSZ-13 under SCR Condition. Environmental Science & Technology, 2022, 56, 1917-1926.	4.6	34
103	A novel Î ³ -like MnO2 catalyst for ozone decomposition in high humidity conditions. Journal of Hazardous Materials, 2021, 420, 126641.	6.5	33
104	High Selectivity to HCl for the Catalytic Removal of 1,2-Dichloroethane Over RuP/3DOM WO _{<i>x</i>} : Insights into the Effects of P-Doping and H ₂ O Introduction. Environmental Science & Technology, 2021, 55, 14906-14916.	4.6	33
105	NO _{<i>x</i>} Removal over V ₂ O ₅ /WO ₃ –TiO ₂ Prepared by a Grinding Method: Influence of the Precursor on Vanadium Dispersion. Industrial & Engineering Chemistry Research, 2018. 57. 150-157.	1.8	32
106	Synthesis of α–MnO2–like rod catalyst using YMn2O5 A–site sacrificial strategy for efficient benzene oxidation. Journal of Hazardous Materials, 2021, 403, 123811.	6.5	32
107	Vanadium-density-dependent thermal decomposition of NH ₄ HSO ₄ on V ₂ O ₅ /TiO ₂ SCR catalysts. Catalysis Science and Technology, 2019, 9, 3779-3787.	2.1	31
108	Effects of dietary vitamin C and vitamin E on the growth, antioxidant defence and digestive enzyme activities of juvenile discus fish (<i>Symphysodon haraldi</i>). Aquaculture Nutrition, 2019, 25, 176-183.	1.1	31

#	Article	IF	CITATIONS
109	Fabrication and Electrochemical Treatment Application of an Al-Doped PbO ₂ Electrode with High Oxidation Capability, Oxygen Evolution Potential and Reusability. Journal of the Electrochemical Society, 2015, 162, E258-E262.	1.3	30
110	A neutral and coordination regeneration method of Ca-poisoned V2O5-WO3/TiO2 SCR catalyst. Catalysis Communications, 2017, 100, 112-116.	1.6	30
111	Promotion Effect of Gaâ^'Co Spinel Derived from Layered Double Hydroxides for Toluene Oxidation. ChemCatChem, 2018, 10, 4838-4843.	1.8	30
112	Rational tuning towards A/B-sites double-occupying cobalt on tri-metallic spinel: Insights into its catalytic activity on toluene catalytic oxidation. Chemical Engineering Journal, 2020, 399, 125792.	6.6	30
113	Fabrication of Nanohybrid Spinel@CuO Catalysts for Propane Oxidation: Modified Spinel and Enhanced Activity by Temperature-Dependent Acid Sites. ACS Applied Materials & Interfaces, 2021, 13, 27106-27118.	4.0	30
114	Boosting nitrous oxide direct decomposition performance based on samarium doping effects. Chemical Engineering Journal, 2021, 414, 128643.	6.6	30
115	New insight on electroreduction of nitrate to ammonia driven by oxygen vacancies-induced strong interface interactions. Journal of Catalysis, 2022, 406, 39-47.	3.1	29
116	Efficient Electron Transfer by Plasmonic Silver in SrTiO ₃ for Low-Concentration Photocatalytic NO Oxidation. Environmental Science & amp; Technology, 2022, 56, 3604-3612.	4.6	29
117	Iron tungsten mixed composite as a robust oxygen evolution electrocatalyst. Chemical Communications, 2019, 55, 10944-10947.	2.2	28
118	Carbon/chlorinate deposition on MnOx-CeO2 catalyst in chlorobenzene combustion: The effect of SCR flue gas. Chemical Engineering Journal, 2022, 433, 133552.	6.6	28
119	Efficient Electrochemical Nitrate Reduction to Ammonia with Copperâ€Supported Rhodium Cluster and Singleâ€Atom Catalysts. Angewandte Chemie, 2022, 134, .	1.6	28
120	The outstanding performance of LDH-derived mixed oxide Mn/CoAlO _x for Hg ⁰ oxidation. Catalysis Science and Technology, 2015, 5, 3536-3544.	2.1	27
121	Nature of active Fe species and reaction mechanism over high-efficiency Fe/CHA catalysts in catalytic decomposition of N2O. Journal of Catalysis, 2020, 392, 322-335.	3.1	27
122	Distinctive Bimetallic Oxides for Enhanced Catalytic Toluene Combustion: Insights into the Tunable Fabrication of Mnâ^'Ce Hollow Structure. ChemCatChem, 2020, 12, 2872-2879.	1.8	27
123	Surface Reconstruction of a Mullite-Type Catalyst via Selective Dissolution for NO Oxidation. ACS Catalysis, 2021, 11, 14507-14520.	5.5	27
124	Simultaneous removal of NOx and chlorobenzene on V2O5/TiO2 granular catalyst: Kinetic study and performance prediction. Frontiers of Environmental Science and Engineering, 2021, 15, 1.	3.3	26
125	The effect of additives and intermediates on vanadia-based catalyst for multi-pollutant control. Catalysis Science and Technology, 2020, 10, 323-326.	2.1	25
126	Modified red mud catalyst for the selective catalytic reduction of nitrogen oxides: Impact mechanism of cerium precursors on surface physicochemical properties. Chemosphere, 2020, 257, 127215.	4.2	25

#	Article	IF	CITATIONS
127	Modified Silica Adsorbents for Toluene Adsorption under Dry and Humid Conditions: Impacts of Pore Size and Surface Chemistry. Langmuir, 2019, 35, 8927-8934.	1.6	24
128	New Insights on Competitive Adsorption of NO/SO ₂ on TiO ₂ Anatase for Photocatalytic NO Oxidation. Environmental Science & Technology, 2021, 55, 9285-9292.	4.6	24
129	Promotion of H ₃ PW ₁₂ O ₄₀ Grafting on NO _{<i>x</i>} Abatement over γ-Fe ₂ O ₃ : Performance and Reaction Mechanism. Industrial & Engineering Chemistry Research, 2018, 57, 13661-13670.	1.8	22
130	Deactivation of Pt-Au/TiO2-CeO2 catalyst for co-oxidation of HCHO, H2 and CO at room temperature: Degradations of active sites and mutual influence between reactants. Applied Catalysis A: General, 2019, 582, 117116.	2.2	22
131	Activity improvement of acid treatment on LaFeO3 catalyst for CO oxidation. Catalysis Today, 2021, 376, 205-210.	2.2	21
132	Facile synthesis λâ€MnO2 spinel for highly effective catalytic oxidation of benzene. Chemical Engineering Journal, 2021, 421, 127828.	6.6	21
133	NH3 selective catalytic reduction of NO: A large surface TiO2 support and its promotion of V2O5 dispersion on the prepared catalyst. Chinese Journal of Catalysis, 2016, 37, 878-887.	6.9	20
134	Quantitative Cu Counting Methodologies for Cu/SSZ-13 Selective Catalytic Reduction Catalysts by Electron Paramagnetic Resonance Spectroscopy. Journal of Physical Chemistry C, 2020, 124, 28061-28073.	1.5	20
135	Severe deactivation and artificial enrichment of thallium on commercial SCR catalysts installed in cement kiln. Applied Catalysis B: Environmental, 2020, 277, 119194.	10.8	20
136	Selective Catalytic Reduction of NO _{<i>x</i>} with NH ₃ over Cu/SSZ-13: Elucidating Dynamics of Cu Active Sites with In Situ UV–Vis Spectroscopy and DFT Calculations. Journal of Physical Chemistry C, 2022, 126, 8720-8733.	1.5	20
137	Novel W-modified SnMnCeO catalyst for the selective catalytic reduction of NO with NH3. Catalysis Communications, 2017, 100, 117-120.	1.6	19
138	Nb-incorporated Fe (oxy)hydroxide derived from structural transformation for efficient oxygen evolution electrocatalysis. Journal of Materials Chemistry A, 2020, 8, 24598-24607.	5.2	18
139	The Roles of Various Plasma Active Species in Toluene Degradation by Non-thermal Plasma and Plasma Catalysis. Plasma Chemistry and Plasma Processing, 2019, 39, 1469-1482.	1.1	17
140	Comparison of NH3-SCO performance over CuOx/H-SSZ-13 and CuOx/H-SAPO-34 catalysts. Applied Catalysis A: General, 2019, 585, 117119.	2.2	17
141	Investigation on removal of NO and HgO with different Cu species in Cu-SAPO-34 zeolites. Catalysis Communications, 2019, 119, 91-95.	1.6	17
142	New Insight into the In Situ SO2 Poisoning Mechanism over Cu-SSZ-13 for the Selective Catalytic Reduction of NOx with NH3. Catalysts, 2020, 10, 1391.	1.6	17
143	Identification of Intrinsic Active Sites for the Selective Catalytic Reduction of Nitric Oxide on Metal-Free Carbon Catalysts via Selective Passivation. ACS Catalysis, 2022, 12, 1024-1030.	5.5	17
144	Effect of Fe precursors on the catalytic activity of Fe/SAPO-34 catalysts for N2O decomposition. Catalysis Communications, 2019, 128, 105706.	1.6	16

#	Article	IF	CITATIONS
145	The promotion effect of ceria on high vanadia loading NH3-SCR catalysts. Catalysis Communications, 2019, 121, 84-88.	1.6	16
146	Metal–Support Interactions within a Dual-Site Pd/YMn ₂ O ₅ Catalyst during CH ₄ Combustion. ACS Catalysis, 2022, 12, 4430-4439.	5.5	16
147	Hierarchically devising NiFeO H catalyst with surface Fe active sites for efficient oxygen evolution reaction. Catalysis Today, 2021, 364, 140-147.	2.2	14
148	Mercury speciation and size-specific distribution in filterable and condensable particulate matter from coal combustion. Science of the Total Environment, 2021, 787, 147597.	3.9	14
149	Insight into the promotion mechanism of activated carbon on the monolithic honeycomb red mud catalyst for selective catalytic reduction of NOx. Frontiers of Environmental Science and Engineering, 2021, 15, 1.	3.3	14
150	Predicting the adsorption of organic pollutants on boron nitride nanosheets <i>via in silico</i> techniques: DFT computations and QSAR modeling. Environmental Science: Nano, 2021, 8, 795-805.	2.2	13
151	Improvement of Al2O3 on the multi-pollutant control performance of NOx and chlorobenzene in vanadia-based catalysts. Chemosphere, 2022, 289, 133156.	4.2	13
152	Activating Surface Lattice Oxygen of a Cu/Zn _{1<i>–x</i>} Cu _{<i>x</i>} O Catalyst through Interface Interactions for CO Oxidation. ACS Applied Materials & Interfaces, 2022, 14, 9882-9890.	4.0	13
153	Influence of sulfation on CeO2-ZrO2 catalysts for NO reduction with NH3. Chinese Journal of Catalysis, 2017, 38, 160-167.	6.9	12
154	Selective Catalytic Reduction of NO _{<i>x</i>} with Ammonia over Copper Ion Exchanged SAPOâ€47 Zeolites in a Wide Temperature Range. ChemCatChem, 2018, 10, 2481-2487.	1.8	10
155	Insights into the binding manners of an Fe doped MOF-808 in high-performance adsorption: a case of antimony adsorption. Environmental Science: Nano, 2022, 9, 254-264.	2.2	10
156	Insights over Titanium Modified FeMgOx Catalysts for Selective Catalytic Reduction of NOx with NH3: Influence of Precursors and Crystalline Structures. Catalysts, 2019, 9, 560.	1.6	9
157	Key intermediates from simultaneous removal of NO _{<i>x</i>} and chlorobenzene over a V ₂ O ₅ –WO ₃ /TiO ₂ catalyst: a combined experimental and DFT study. Catalysis Science and Technology, 2021, 11, 7260-7267.	2.1	9
158	Carbon Dioxide Promotes Dehydrogenation in the Equimolar C 2 H 2 O 2 Reaction to Synthesize Carbon Nanotubes. Small, 2018, 14, 1703482.	5.2	8
159	Synergistic Effects of a CeO ₂ /SmMn ₂ O ₅ –H Diesel Oxidation Catalyst Induced by Acid-Selective Dissolution Drive the Catalytic Oxidation Reaction. ACS Applied Materials & Interfaces, 2022, 14, 2860-2870.	4.0	8
160	Dual Active Centers Bridged by Oxygen Vacancies of Ruthenium Singleâ€Atom Hybrids Supported on Molybdenum Oxide for Photocatalytic Ammonia Synthesis. Angewandte Chemie, 2022, 134, .	1.6	8
161	Balancing redox and acidic properties for optimizing catalytic performance of SCR catalysts: A case study of nanopolyhedron CeO -supported WO. Journal of Environmental Chemical Engineering, 2021, 9, 105828.	3.3	7
162	Lean NO –SnO2–CeO2 catalyst at low temperatures. Catalysis Today, 2015, 258, 556-563.	2.2	6

#	Article	IF	CITATIONS
163	Sacrificial carbon strategy for facile fabrication of highly-dispersed cobalt-silicon nanocomposites: Insight into its performance on the CO and CH4 oxidation. Journal of Cleaner Production, 2021, 278, 123920.	4.6	6
164	A dual-functional MnO2/La0.6Sr0.4MnO3 composite catalyst: high-efficiency for elemental mercury oxidation in flue gas. Catalysis Communications, 2018, 112, 43-48.	1.6	4
165	Cerium-tungsten oxides supported on activated red mud for the selective catalytic reduction of NO. Green Energy and Environment, 2023, 8, 173-182.	4.7	4
166	Preparation of <i>γ</i> â€Fe ₂ O ₃ Catalysts and their deNO <i>_x</i> Performance: Effects of Precipitation Conditions. Chemical Engineering and Technology, 2018, 41, 1019-1026.	0.9	2
167	Application of Nanotechnology in Pollution Control of NOx From Stationary Sources. , 2019, , 179-211.		2